Acta metall. mater. Vol. 41, No. 10, pp. 2825–2832, 1993
Printed in Great Britain.

0956-7151/93 $6.00 + 0.00

TEXTURE INFLUENCE ON THE FREQUENCY OF OCCURRENCE OF CSL-BOUNDARIES IN POLYCRYSTALLINE MATERIALS

A. MORAWIEC[1], J. A. SZPUNAR[2] and D. C. HINZ[2]

[1]Instytut Podstaw Metalurgii PAN, 30-059 Kraków, ul. Reymonta 25, Poland and [2]Department of Mining and Metallurgical Engineering, McGill University, Montreal, Quebec, Canada H3A 2T5

(Received 6 November 1992; in revised form 26 March 1993)

Abstract—The influence of crystallographic texture on the frequencies of CSL grain boundaries in polycrystalline materials was investigated. Assuming a spatially disordered material, the explicit relation between these frequencies and the orientation distribution function is given. Also the frequencies of CSL-boundaries with respect to a specified orientation are analyzed and the role of sample symmetry is discussed. Exemplary results obtained for the case of primary recrystallized Fe–3% Si alloy with cubic-orthorhombic symmetry are presented.

Résumé—L'influence de la texture cristallographique sur la fréquence des joints de grains CSL dans les matériaux polycrystallins est analysée. Considérant l'hypothèse selon laquelle le matéiau est désordonné spatialement, il existe une relation existant entre cette fréquence et la fonction de distribution d'orientation. Ainsi, la fréquence des joints CSL pour une orientation donnée est analyseé et l'influence de la symmétrie d'échantillon est discutée. Certains résultats sont présentés pour le cas d'un énchantillon Fe–3% Si recristallisé avec la symmétrie cubique-orthorombique.

Zusammenfassung—Der Einfluß kristallografischer Texturen auf das Auftrefen von CSL-Korngrenzen in polykristallinen Materialen wird untersucht. Unter Annahme eines räumlich ungeordneten Materials wird das Verhältnis zwischen diesem Auftrefen und der Orientierungs-verteilungsfunktion explizit angegeben. Darüberhinaus wird das Auftrefen von CSL-Korngrenzen hinsichtlich einer speziellen Orientierung analysiert und der Einfluß der Probensymmetrie diskutiert. Als Beispiel werden Resultate dargestellt, die in einer primärrekristallisierten Fe–3% Si-Legierung mit kubisch-orthorombishcer Symmetrie erhalten wurden.

INTRODUCTION

Recent studies indicate that the character of grain boundaries influences the properties of polycrystalline materials. Special interest is paid to CSL-boundaries, i.e. boundaries between grains with misorientation close to low-Σ coincidence site lattice positions. It is known that their geometrical features lead to special physical properties. Low-Σ CSL-boundaries, in comparison to general boundaries, are considered to have lower energy, lower intrinsic electrical resistivity, greater resistance to grain-boundary fracture and cavitation, and to the initiation of localized corrosion. A more comprehensive list of special properties of low-Σ CSL-boundaries is available [1].

Some authors [2–4] consider CSL-boundaries important for the case of grain growth in the presence of precipitates. It is believed that precipitation occurs selectively and so distinguishes some low-Σ CSL-boundaries. This makes these boundaries more mobile and, subsequently, influences the structure and properties of the final material.

The frequency of occurrence of CSL-boundaries in a material is influenced by most of the specific features of the microstructure: orientation distribution (texture), correlation between orientations of neighbouring grains, all types of inhomogeneities (bands of different kinds, clusters of grains) and also grain size distribution and its correlation with grain orientation.

We limit our investigation to the influence of texture on the frequency of CSL-boundaries and accordingly neglect the influence of all spatial relations. Hence we ignore inhomogeneities, clustering, orientation correlations and grain size effects. A polycrystal satisfying such assumptions would be rather similar to the perfectly disordered material of Kröner [5], composed of oriented but pointwise grains (hence each of the same size), chaotically scattered throughout the sample to avoid correlations between neighbouring orientations and provide statistical homogeneity. The only difference is that a non-trivial texture is allowed.

Similar analyses have been performed by Garbacz and Grabski [6] and as well by Gertsman *et al.* [7]. Both based their conclusions on axial textures chosen without connection to any particular materials. Our aim is to consider real textures, which are related to abnormal grain growth in Fe–3% Si alloy. Typical

experimental values for the sharpness and the usual cubic-orthorhombic symmetry will be taken into account.

In order to introduce the notation which will be used, let us recall some basic information about the description of texture and its associated symmetries. The crystallite's orientation is specified by an element, say g, of the rotation group SO(3). Texture is usually identified with the orientation distribution function $f:\mathrm{SO}(3)\to\mathbb{R}_+$. It is understood that a random (uniform) orientation distribution corresponds to $f(g)=1$, for all $g\in\mathrm{SO}(3)$. Moreover, the texture function is assumed to be normalized—i.e. the invariant integral of f over SO(3) is unity

$$\int_{\mathrm{SO}(3)} f(g)\mathrm{d}g = 1.$$

Because of crystal symmetry a particular orientation corresponds to several equivalent elements of SO(3). The subgroup of crystal point symmetries containing only proper rotations will be denoted by C. The orientation distribution function thus satisfies the conditions

$$f(c_i g)=f(g), \quad c_i\in C, \quad g\in\mathrm{SO}(3). \tag{1}$$

Moreover, for some orientation distribution functions, there exist elements $s_k\in\mathrm{SO}(3)$ such that

$$f(gs_k)=f(g), \quad \text{for all } g\in\mathrm{SO}(3). \tag{2}$$

The elements s_k satisfying the above condition constitute a subgroup S of SO(3) called the sample symmetry group. Both groups C and S are assumed here to be finite with orders N_C and N_S, respectively.

FREQUENCY OF OCCURRENCE OF CSL-BOUNDARIES

The coincidence site relationship is fully described by the misorientation ("difference" in orientations) between neighbouring grains. Therefore the analysis of CSL-boundaries is governed by special misorientations. Let us consider then the distribution of misorientations between each pair of neighbouring grains, neglecting any spatial relationships and correlations between them. Such a distribution is given by

$$m(g)=\int_{\mathrm{SO}(3)} \mathrm{d}g_0 f(g_0)f(gg_0). \tag{3}$$

The relations (1) and the invariance of the integral over SO(3) lead to the following symmetry conditions

$$\begin{aligned} m(c_i g c_j) &= \int_{\mathrm{SO}(3)} \mathrm{d}g_0 f(g_0)f(c_i g c_j g_0) \\ &= \int_{\mathrm{SO}(3)} \mathrm{d}(c_j g_0) f(c_j g_0) f(g c_j g_0) \\ &= m(g). \end{aligned} \tag{4}$$

For grain boundary analysis, misorientation is symmetric for two neighbouring grains—i.e. grains having orientations g_1 and g_2 imply both $g:=g_1 g_2^{-1}$ and $g_2 g_1^{-1}=g^{-1}$ as misorientations. Therefore, instead of m we are rather interested in the symmetrized function

$$M(g)=\tfrac{1}{2}[m(g)+m(g^{-1})]. \tag{5}$$

Obviously, $M(g^{-1})=M(g)$ and $M(c_j g c_j)=M(g)$, $c_i, c_j\in C$.

To calculate the probability of occurrence of special misorientations one must assume an accuracy criterion. The convention can be made that a misorientation g coincides with a special misorientation g_v if it is sufficiently close to at least one of the points symmetrically equivalent to g_v or g_v^{-1}. More precisely, it occurs if the smallest angle among $\Omega(g(c_i g_v c_j)^{-1})$ and $\Omega(g(c_i g_v^{-1} c_j)^{-1})$, $c_i, c_j\in C$, is smaller than the specified angle ω_v, where $\Omega(g)$ is the rotation angle corresponding to g. It means that g should belong to the sphere centred at the point symmetrically equivalent to g_v or g_v^{-1} and having radius ω_v: $g\in B(c_i g_v c_j, \omega_v)$ or $g\in B(c_i g_v^{-1} c_j, \omega_v)$. Hence the frequency F^v of misorientations denoted g_v is given by

$$F^v=\int_{B_v} \mathrm{d}g M(g),$$

$$B_v:=\bigcup_{i,j=1}^{N_C} [B(c_i g_v c_j, \omega_v)\cup B(c_i g_v^{-1} c_j, \omega_v)]. \tag{6}$$

One can estimate F^v for the special case of a random orientation distribution. Because $f(g)=1$, $g\in\mathrm{SO}(3)$ then $M(g)=1$, $g\in\mathrm{SO}(3)$ and hence

$$\begin{aligned} F^v &= \int_{B_v} \mathrm{d}g \\ &= \sum_{i,j=1}^{N_C} \int_{B(c_i g_v c_j, \omega_v)\cup B(c_i g_v^{-1} c_j, \omega_v)} \mathrm{d}g \\ &= K(g_v)\int_{B(g_v,\omega_v)} \mathrm{d}g, \end{aligned} \tag{7}$$

where partial overlapping of spheres was neglected. $K(g_v)$ is the number of different points within the set $\{g\in\mathrm{SO}(3)\mid g=c_i g_v c_j \text{ or } g=c_i g_v^{-1} c_j,\ c_i, c_j\in C\}$—i.e. the set of points symetrically equivalent to g_v and to g_v^{-1}. It is easy to calculate the integral in (7). Using parameters ϑ, ψ as the polar coordinates of the rotation axis and ω as the rotation angle one has $\mathrm{d}g=(2\pi^2)^{-1}\sin^2(\omega/2)\sin\vartheta\,\mathrm{d}\vartheta\,\mathrm{d}\psi\,\mathrm{d}\omega$, hence

$$\int_{B(g_v,\omega_v)} \mathrm{d}g = \pi^{-1}(\omega_v-\sin\omega_v). \tag{8}$$

Now for $K(g_v)$, the highest possible value is $2N_C^2$. The overlapping of points symmetrically equivalent to g_v means that $c_i g_v c_j=g_v$ for some $c_i, c_j\in C$. Let $N(g_v)$ be the number of unique pairs $(c_i, c_j)\in C\times C$ satisfying this relation. Then the number of different points symmetrically equivalent to g_v equals $N_C^2/N(g_v)$. The same takes place for g_v^{-1}. Moreover, it is possible to verify that if overlapping occurs for two points $c_i g_v c_j$ and $c_k g_v^{-1} c_l$, then any point symmetrically equivalent to g_v will overlap with a point

symmetrically equivalent to g_v^{-1}. Let $\lambda_v = 1$ in such a case, $\lambda_v = 2$ otherwise. Summarizing

$$F^v = \frac{\lambda_v N_C^2}{\pi N(g_v)}(\omega_v - \sin\omega_v). \tag{9}$$

Let the special misorientations be defined as those satisfying CSL relations for low Σ—i.e. $v = \Sigma$. Let us restrict ourselves to materials of cubic symmetry ($N_C = 24$) and Σ up to 51. Following other papers on this subject we assume the Brandon's accuracy criterion: $\omega_\Sigma = 15^\circ/\sqrt{\Sigma}$. The numbers $N(g_\Sigma)$ of overlapping points are given in Table 1. The coefficient λ_Σ equals 1 for all Σ except $\Sigma = 39b$ and $\Sigma = 51c$: $\lambda_{39b} = \lambda_{51c} = 2$. Using this and equation (9) one obtains the frequencies F^Σ listed in Table 1.

Table 1. Frequencies of occurrence of low-Σ CSL misorientation relationships

Σ	$N(g_\Sigma)$	$100 \times F^\Sigma$	4	5	6	7
1	24	2.2768		2.32	3.86	3.81
3	6	1.7567		1.81	1.94	0.27
5	4	1.2252		1.18	0.93	2.98
7	3	0.9864		0.98	1.07	0.57
9	2	1.0150		1.07	1.01	0.97
11	2	0.7512		0.76	0.75	0.41
13*a*	4	0.2924		0.30	0.28	0.39
13*b*	3	0.3898		0.43	0.49	0.44
15	1	0.9436		0.99	0.78	0.69
17*a*	4	0.1955		0.20	0.16	0.26
17*b*	2	0.3911	0.389	0.39	0.44	0.18
19*a*	2	0.3310		0.32	0.40	0.46
19*b*	3	0.2206		0.23	0.24	0.04
21*a*	3	0.1899		0.19	0.25	0.26
21*b*	1	0.5697		0.57	0.52	0.27
23	1	0.4970		0.53	0.39	0.61
25*a*	4	0.1096		0.10	0.16	0.13
25*b*	1	0.4386		0.46	0.36	0.34
27*a*	2	0.1954		0.19	0.20	0.29
27*b*	1	0.3908		0.38	0.38	0.70
29*a*	4	0.0870	0.074	0.07	0.06	0.32
29*b*	1	0.3511		0.36	0.37	0.13
31*a*	3	0.1059		0.10	0.16	0.15
31*b*	1	0.3176		0.29	0.32	0.14
33*a*	2	0.1446		0.15	0.18	0.18
33*b*	1	0.2892		0.26	0.32	0.38
33*c*	2	0.1446		0.15	0.17	0.02
35*a*	1	0.2648		0.25	0.32	0.34
35*b*	1	0.2648		0.26	0.26	0.14
37*a*	4	0.0609		0.07	0.07	0.09
37*b*	1	0.2436		0.24	0.22	0.45
37*c*	3	0.0812		0.07	0.09	0.02
39*a*	3	0.0750		0.08	0.08	0.06
39*b*	1	0.4502		0.46	0.45	0.24
41*a*	2	0.1044		0.11	0.18	0.15
41*b*	1	0.2088		0.23	0.20	0.28
41*c*	2	0.1044		0.09	0.11	0.04
43*a*	3	0.0648		0.05	0.10	0.11
43*b*	1	0.1944		0.19	0.17	0.27
43*c*	2	0.0972		0.10	0.11	0.02
45*a*	1	0.1816		0.18	0.17	0.30
45*b*	1	0.1816		0.18	0.20	0.16
45*c*	1	0.1816		0.19	0.19	0.10
47*a*	1	0.1702		0.18	0.17	0.16
47*b*	1	0.1702		0.19	0.15	0.22
49*a*	3	0.0533		0.05	0.06	0.03
49*b*	1	0.1598		0.16	0.12	0.36
49*c*	1	0.1598		0.14	0.14	0.05
51*a*	2	0.0753		0.08	0.12	0.08
51*b*	2	0.0753		0.07	0.10	0.11
51*c*	1	0.3011		0.33	0.25	0.20
$100 \times (1 - \Sigma F^\Sigma)$		81.4684	81.482			
Overlapping			+1.269			
General boundaries			82.751	82.570	81.21	82.02

Column 4 contains corrections to formulae (9) due to overlapping. Computed results based on 10^5 points for a random texture and for the texture displayed in Fig. 2 are given in columns 5 and 6 respectively. Column 7 contains frequencies of CSL-misorientations with respect to the Goss position for the texture of Fig. 2. The number of points generated in the last case is 25,000. All frequencies are multiplied by 100—i.e. percentages are given.

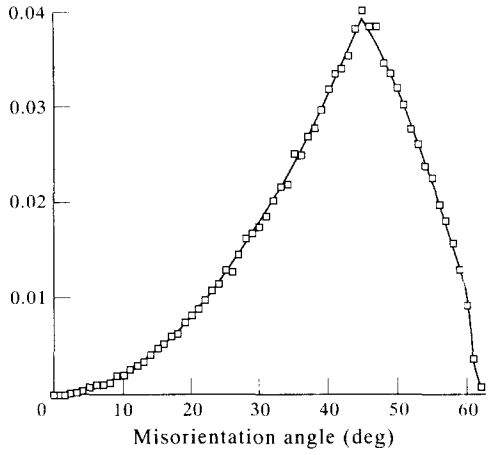

Fig. 1. Theoretical (line) and calculated (squares) misorientation angle distributions.

The results, corrected to take into account that 0.25 rad $\neq 15^\circ$, coincide with those published by Warrington and Boon [8] (up to $\Sigma = 25$) except $\Sigma = 11$. They agree also with results given by Palumbo and Aust [9] (up to $\Sigma = 49$) except $\Sigma = 21$, 39, 41.

As we have already alluded there can also occur partial overlapping of spheres. For spheres corresponding to the same Σ, it takes place in two cases: $\Sigma = 17b$ and $\Sigma = 29a$ ($\Sigma \leqslant 51$). Therefore, these two results have to be modified. In both cases there occur pairs of partially overlapping spheres. The distances between centres are 6.743° for $\Sigma = 17b$ and 2.800° for $\Sigma = 29a$ with the corresponding diameters of spheres obtained from Brandon's criterion being $2\omega_{17b} = 7.276^\circ$ and $2\omega_{29a} = 5.571^\circ$. Because of this partial overlapping the frequencies of $\Sigma = 17b$ and $\Sigma = 29a$ boundaries obtained from equation (9) have to be reduced by factors 0.9955 and 0.8454, respectively. [The approximation $\omega - \sin\omega \cong \omega^3/6$ was used to estimate the volumes of overlapping regions.] The modified values are given in the fourth column of Table 1.

To calculate the fraction of misorientations not covered by low-Σ CSL spheres one usually subtracts the summed low-Σ frequencies from the total volume of SO(3) (equal to 1). This procedure does not include the overlap occurring between spheres corresponding to different Σ. The quantitative value of the underestimation due to overlap of this kind is 0.0127.

To obtain the frequencies of special misorientations for non-random textures computer calculations must be performed. The procedure involves generating pairs of orientations in such a way that their total distribution agrees with the assumed texture function. It is then verified whether the difference in orientation

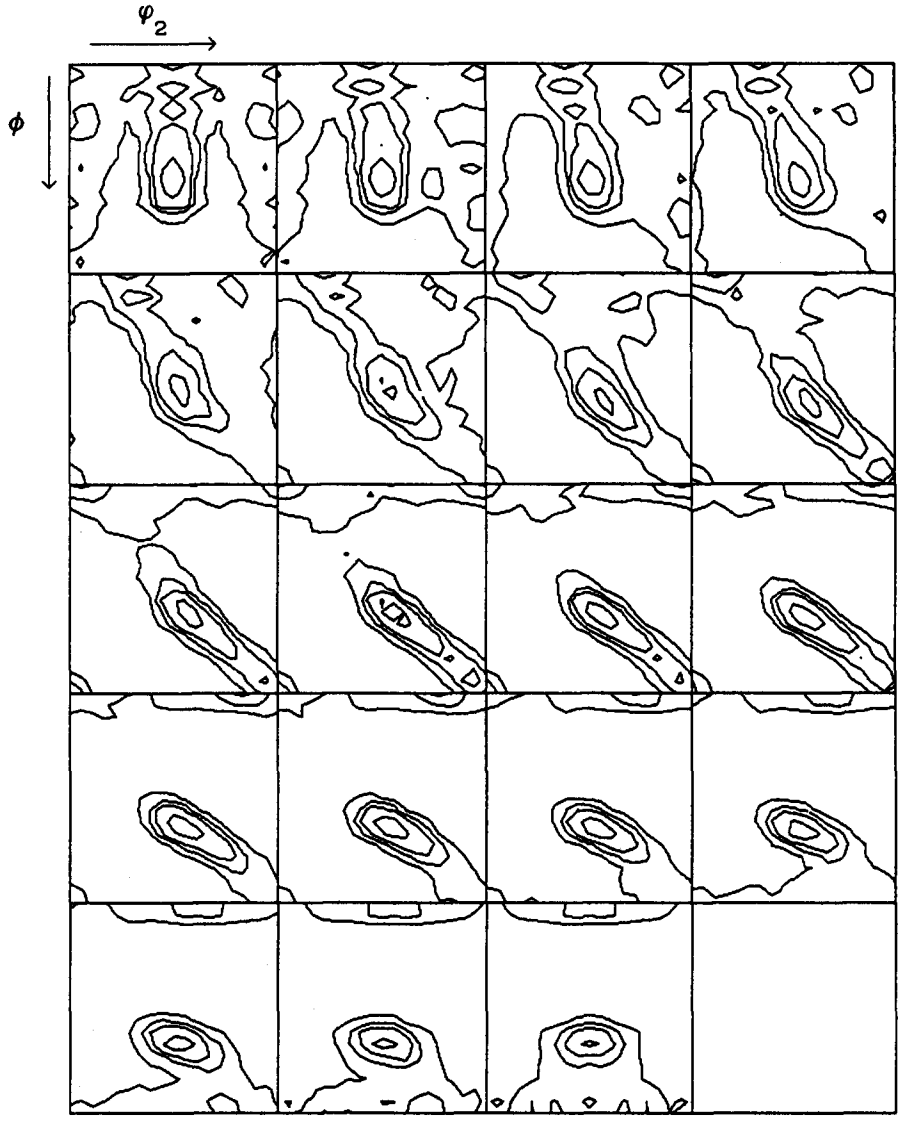

Fig. 2. Normalized orientation distribution function of primary recrystallized Fe–3% Si alloy. The levels are 1, 2, 3 and 5. Background and maximum equal 0.05 and 6.81 respectively. The standard coordinates $(\varphi_1, \phi, \varphi_2)$ [13] are used in the φ_1 projection.

is close enough to any of the specified low-Σ misorientations.

The frequencies obtained for a random orientation distribution using this program are given in the fifth column of Table 1. The number of generated misorientations is 10^5. The results agree well with those of column four, the relative error being 6.16%. Also, the calculated distribution of misorientation angle was compared to the theoretical one [10–12] and both are shown in Fig. 1. Additionally, for comparison the frequencies of CSL-boundaries were calculated for some of the fibre textures given by Garbacz and Grabski [6]. The results obtained are similar to those they reported.

The conclusion of Garbacz and Grabski [6] (as well as Gertsman *et al.* [7]) was that texture strongly influences the frequencies of CSL-boundaries. But the hypothetical textures considered there were extraordinarily sharp. In our case the calculations are carried out for the real texture of primary recrystallized Fe–3% Si alloy (Fig. 2)†. The results are given in column six of Table 1 and in Fig. 3. One can notice that for this texture the frequencies are close to those corresponding to a random orientation distribution. Therefore in this case, texture is rather a weak or even negligible factor.

The curve in Fig. 4 illustrates how the sharpness of texture influences the frequency of CSL-boundaries. The difference in frequencies of CSL-misorientation relationships between random and non-random

†Dr P. Gangli is acknowledged for allowing us to use experimental pole figures. The presented texture function was calculated using a program written by one of the authors (A.M.).

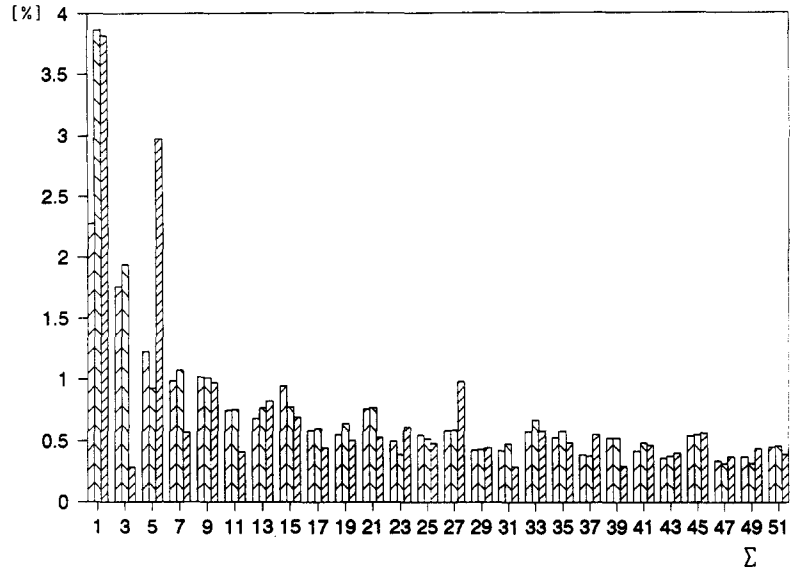

Fig. 3. The frequencies of CSL-misorientations: first bar-theoretical result for a random orientation distribution, second bar-result corresponding to the texture displayed in Fig. 2 (column 6 of Table 1), third bar-frequencies of CSL-misorientations with respect to the Goss position for the texture of Fig. 2 (column 7 of Table 1).

textures is characterized by

$$D := \sum_{\Sigma=1}^{27b} (\text{frequency}(\Sigma, f) - \text{frequency}(\Sigma, \text{random}))^2$$

and the quatity $\int_{SO(3)}[f(g)-1]^2\,dg$ (=texture index -1) represents the texture sharpness. The textures used for the calculations are similar to that shown in Fig. 2—i.e. they consist of the so-called γ-fibre ($\varphi_2 = 45°$, $\phi = 55°$, $\varphi_1 \in [0°, 90°]$) with increasing sharpness. The curve confirms the obvious fact that boundary character is strongly influenced by sharp textures but slightly influenced by weak or moderate textures. Textures of Fe–3% Si alloys which result from primary recrystallization belong to the latter category and thus one cannot expect strong preferences for CSL-boundaries based on non-random orientation distributions.

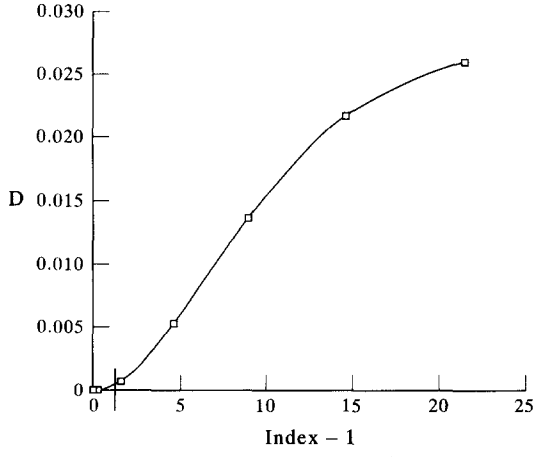

Fig. 4. Dependence of the frequencies of CSL-misorientation relationships on texture sharpness. The long tic mark on the abssissa corresponds to the exemplary texture (Fig. 2).

FREQUENCY OF OCCURRENCE OF CSL-BOUNDARIES WITH RESPECT TO A SPECIFIED ORIENTATION

Previously, the frequencies of occurrence of CSL-boundaries were considered generally, without reference to any specific orientation. Some orientations, however, play special roles in texture evolution. It is thus of interest to discuss how often grains with such orientations have low-Σ CSL-boundaries arising from the texture of a material, or in other words, how frequently do grains have a misorientation g with respect to a specified orientation g_0. According to our original assumptions it is represented by the probability of occurrence of the orientation gg_0, namely $f(gg_0)$. Because the same crystal orientation is represented by N_C points $c_i g_0$ of SO(3), we define

$$m_{g_0}(g) = \frac{1}{N_C} \sum_{i=1}^{N_C} f(g c_i g_0). \tag{10}$$

From this definition and from $f(c_i g) = f(g)$ follow the results that $m_{c_j g_0} = m_{g_0}$ and $m_{g_0}(c_i g c_j) = m_{g_0}(g)$, $c_i, c_j \in C$. The function m_{g_0}, contrary to the previous function m, is influenced also by the statistical symmetry of the sample—i.e. on the basis of relations (2) one has $m_{g_0 s_k} = m_g$, $s_k \in S$.

Again, of more importance for us is the function symmetrized with respect to g and g^{-1}

$$M_{g_0}(g) := \tfrac{1}{2}[m_{g_0}(g) + m_{g_0}(g^{-1})]. \tag{11}$$

The symmetry properties of M_{g_0} are analogous to those of m_{g_0}—i.e. $M_{c_l g_0 s_k}(c_l g c_j) = M_{g_0}(g)$. It is worth

noticing that the function m, given by definition (3), at point g, is just the average of $m_{g_0}(g)$ weighted according to $f(g_0)$

$$m(g) = \int_{SO(3)} dg_0 f(g_0) m_{g_0}(g). \tag{12}$$

In this sense m_{g_0} is more basic than the function m. The same conclusion can be drawn between M_{g_0} and M.

The frequency of occurrence of a special misorientation g_v with respect to g_0 is given by a relation analogous to (6)

$$F^v_{g_0} = \int_{B_v} dg M_{g_0}(g). \tag{13}$$

For a random orientation distribution this frequency is insensitive to g_0, so that $F^v_{g_0} = F^v$ in this case.

The results for the non-trivial texture shown in Fig. 2 with g_0 being the Goss position ($\varphi_1 = 90°$, $\phi = 90°$, $\varphi_2 = 45°$) are given in the seventh column of Table 1 and in Fig. 3. Although they are more distinct from the random case than those given in the sixth column of Table 1, the differences for most of the Σ are not very significant. The most obvious differences are the supression of the $\Sigma = 3$ misorientation relationship and the relatively high frequency of $\Sigma = 5$. One can also observe the presence of $\Sigma = 27$ and the lack of $\Sigma = 7$ and $\Sigma = 11$.

The frequencies of low-Σ misorientations were also calculated for other points on the η-fibre ($\varphi_1 \in 90°$, $\phi = 90°$, $\varphi_2 \in [0°, 90°]$) appearing in the intermediate stage of texture evolution in Fe–3% Si alloy. The results for $\Sigma = 3$, 5, 7 and 9 are given in Fig. 5. One can notice that the frequency of $\Sigma = 3$ is low along the fibre. The $\Sigma = 9$ relationship, which sometimes is considered to be important, does not exhibit any characteristic features. The frequency of $\Sigma = 5$ is above its random value and has a relatively strong maximum at the Goss position. On the other hand, $\Sigma = 7$ has a minimum at this point (below the random value) and a maximum (above the random value) at $\varphi_2 = 20°$ along with the symmetrically equivalent point $\varphi_2 = 70°$.

Because of sample symmetry some points which can be chosen as g_0 have a special property. Let's consider pairs $(c_i, s_k) \in C \times S$ which preserve the point g_0—i.e. $c_i g_0 s_k = g_0$. The number of such pairs will be called here the multiplicity of the point g_0. For most orientations this value is equal to 1 but there are some with higher multiplicity. Following the extremal example in the Appendix, one can check that an orientation g_0 which is in a misorientation relationship g_v with respect to an orientation g_x, generally is not in the same misorientation relationship to the complementary points $g_x s_k$, $s_k \neq I$ (I – unit matrix). Exceptions from this rule are points g_0 having a

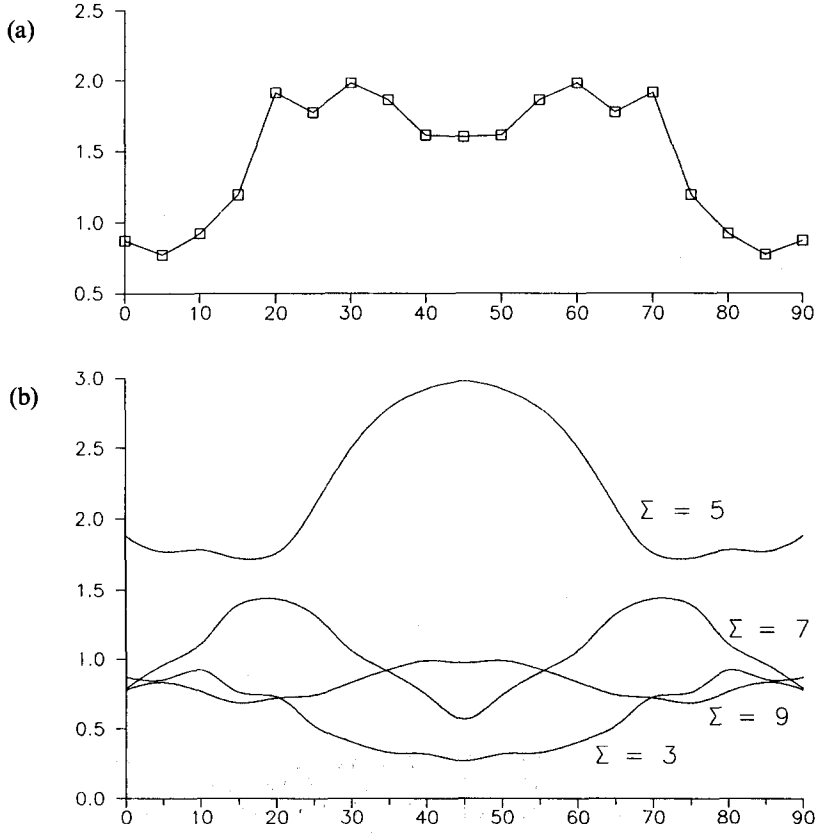

Fig. 5.(a) Skeleton line along the η-fibre. (b) Frequency of occurrence of the low-Σ CSL misorientation relationships with respect to the points on the η-fibre.

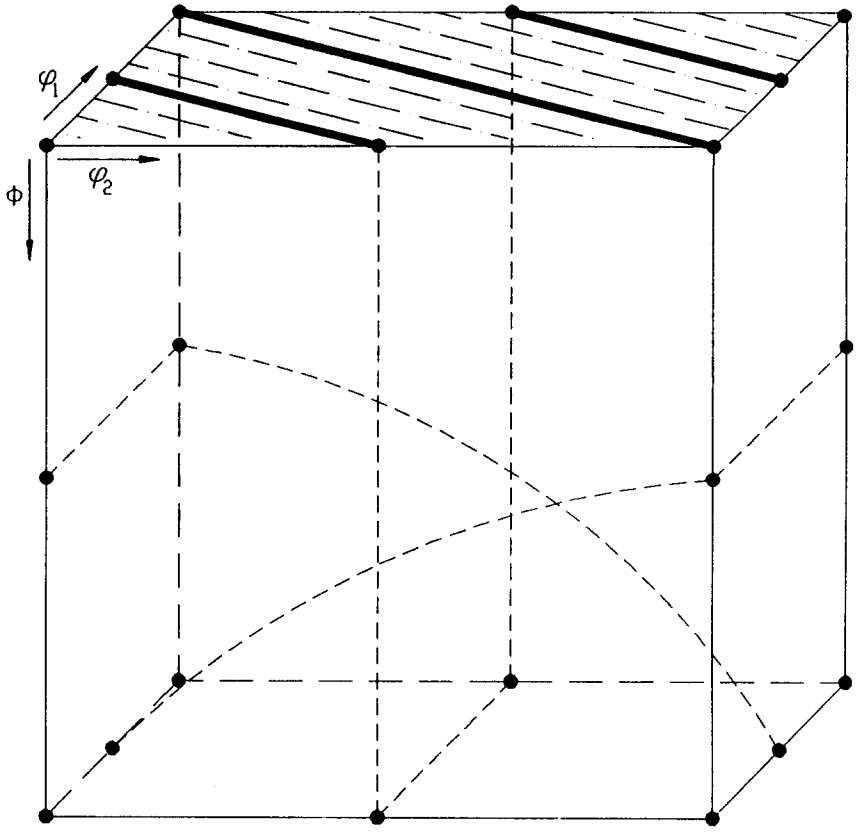

Fig. 6. Orientations with high multiplicity for cubic-orthorhombic symmetry. Points on all thin lines, continuous and dashed, have multiplicity of 2. Points with multiplicity of 4 are marked by thick lines and dots.

higher multiplicity factor. It follows that a higher multiplicity of g_0 leads to a higher possible maximal value of $F^{v}_{g_0}$. When the texture is sharper, the effect is stronger.

The process of grain growth depends on many factors. However, one can notice that orientations characterized by high multiplicity appear often in this problem. In our exemplary case of Fe–3% Si alloy, the texture during grain growth develops in such a way that components present after primary recrystallization vanish and the η-fibre (multiplicity 2) grows, followed by a subsequent rearrangement leading to a dominant Goss component (multiplicity 4). Generally, the most interesting recrystallization textures have components with high multiplicity.

FINAL REMARKS

The program developed allows to investigate the relationship between texture and the presence of special misorientations; in particular case, misorientations characterizing low-Σ CSL-boundaries. The basic assumption is the absence of spatial correlations between orientations and of correlations between orientation and spatial features of a grain.

Although the frequency of CSL-boundaries depends on texture, the preferences are not significant for textures which are not sharp. To this class belong textures of primary recrystallized Fe–3% Si alloys. Therefore, in this case, boundary character distributions based on texture are close to those corresponding to a random (uniform) orientation distribution.

Acknowledgement—This work was supported by the Natural Sciences and Engineering Research Council of Canada.

REFERENCES

1. K. T. Aust and G. Palumbo, in *Structure and Property Relationships for Interfaces* (edited by J. L. Walter *et al.*). A.S.M., Metals, Park, Ohio (1991).
2. J. Harase, R. Shimizu and T. Watanabe, *Proc. 7th Int. Symp. on Metallurgy and Materials Science*, Risø, Denmark, p. 343 (1986).
3. J. Harase and R. Shimizu, *Trans. Japan Inst. Metals* **29**, 388 (1988).
4. N. Rouag, G. Vigna and R. Penelle, *Acta metall. mater.* **38**, 1101 (1990).
5. E. Kröner, *J. Mech. Phys. Solids* **15**, 319 (1967).
6. A. Garbacz and M. W. Grabski, *Scripta metall.* **23**, 1369 (1989).
7. V. Yu. Gertsman, A. P. Zhilyaev, A. I. Pshenichnyuk and R. Z. Valiev, *Acta metall. mater.* **40**, 1433 (1992).
8. D. H. Warrington and M. Boon, *Acta metall.* **23**, 599 (1975).
9. G. Palumbo and K. T. Aust, in *Recrystallization '90* (edited by T. Chandra). IMS (1990).
10. J. K. McKenzie and M. J. Thomson, *Biometrika* **44**, 205 (1957).

11. J. K. McKenzie, *Biometrika* **45**, 229 (1958).
12. D. C. Handscomb, *Can. J. Math.* **10**, 85 (1958).
13. H. J. Bunge, *Texture Analysis in Material Science*. Butterworths, London (1982).

APPENDIX

To show how multiplicity influences the frequency of special misorientations let us consider a texture with only one extremely sharp component at point g_x

$$f(g)=\frac{1}{N_C N_S}\sum_{i=1}^{N_C}\sum_{k=1}^{N_S}\delta(g, c_i g_x s_k) \tag{A1}$$

For simplicity it was assumed that the multiplicity of g_x is 1 and that the misorientation g_v, of which we are interested, corresponds to $\lambda_v = 1$ like most CSL misorientations listed in Table 1.

According to definition (10), the corresponding m_{g_0} function is given by

$$m_{g_0}(g)=\frac{1}{N_C^2 N_S}\sum_{i,j=1}^{N_C}\sum_{k=1}^{N_S}\delta(g, c_i g_x s_k g_0^{-1} c_j). \tag{A2}$$

Now we find the frequency $F_{g_0}^v$ for $g_0 = g_v^{-1} g_x$. Let the symmetry conditions be such as to allow the multiplicity of g_0 to be equal to N_S (as it is in the case of cubic-orthorhombic symmetry). It means that for each $s_k \in S$ there exists $c_l \in C$ such that $s_k g_0^{-1} = g_0^{-1} c_l$. Therefore all the points $c_i g_x s_k g_0^{-1} c_j$, $i, j = 1, \ldots, N_C$ $k = 1, \ldots, N_S$ coincide with the misorientations $c_i g_x g_0^{-1} c_l = c_i g_v c_l$ symmetrically equivalent to g_v. Hence

$$F_{g_0}^v = 1. \tag{A3}$$

On the other hand, if the multiplicity of g_0 equals 1 and no additional overlapping occurs (i.e. $c_i g_x s_k g_0^{-1} c_j \neq g_x g_0^{-1}$ for $s_k \neq I$) then

$$F_{g_0}^v = \frac{1}{N_S}. \tag{A4}$$

In other words, the reference orientation g_0 can be in a given misorientation relationship g_v with respect to g_x but it does not necessarily have to be in the same relationship to the complementary points $g_x s_k$, $s_k \neq I$. This is the case if g_0 has a multiplicity N_S. One can notice that an analogous result follows for the exchanged roles of g_0 and g_x.

For cubic-orthorhombic symmetry, points of the highest multiplicity (equal to 4) are displayed together with points of multiplicity 2 in Fig. 6. The formulae for the curve lines are

$$\varphi_1 = \arccos\left(\frac{\cos(\chi)}{t(\chi)}\right),$$

$$\phi = \arccos\left(\frac{\sqrt{2}}{2}\sin(\chi)\right),$$

$$\phi_2 = \arccos\left(\frac{\sin(\chi)}{t(\chi)}\right) \tag{A5}$$

and

$$\varphi_1 = \arccos\left(\frac{1}{t(\chi)}\right),$$

$$\phi = \arccos\left(\frac{\sqrt{2}}{2}\sin(\chi)\right),$$

$$\varphi_2 = \arcsin\left(\frac{\sin(\chi)}{t(\chi)}\right), \tag{A6}$$

where $t(\chi) := \sqrt{(1+\cos^2\chi)}$ and $\chi \in [0, \pi/2]$.

One can check that the curves (18) and (19) lie on the surfaces $\cos\varphi_2 = \cot\phi$ and $\sin\varphi_2 = \cos\phi$ respectively, dividing the cube $\varphi_1, \phi, \varphi_2 \in [0°, 90°]$ into symmetrically equivalent volumes (see e.g. [13]).